P H Y S I C A L R E V I E W L E T T E R S

Nonresonant Inelastic X-Ray Scattering Involving Excitonic Excitations: The Examples of NiO and CoO

M. W. Haverkort,[1] A. Tanaka,[2] L. H. Tjeng,[1] and G. A. Sawatzky[3]

[1]*II. Physikalisches Institut, Universität zu Köln, Zülpicher Strasse 77, D-50937 Köln, Germany*
[2]*Department of Quantum Matter, ADSM, Hiroshima University, Higashi-Hiroshima 739-8530, Japan*
[3]*Department of Physics and Astronomy, University of British Columbia, Vancouver, British Columbia, Canada V6T 1Z1*

In a recent publication Larson *et al.* reported remarkably clear *d-d* excitations for NiO and CoO with x-ray scattering. Here we present an accurate quantitative description based on a local many body approach, beyond local density approximation + Hubbard U approximations. The magnitude of $\vec{q}$ determines which of the allowed multipoles contributes most to the spectra. The direction of $\vec{q}$ with respect to the crystal can be used as an equivalent to polarization similar to electron energy loss spectroscopy, allowing for a determination of the local symmetry of the initial and final states. This method is more generally applicable and could be a powerful tool for the study of local distortions and symmetries in transition metal and rare earth compounds.

Transition metal compounds with partially filled *d* shells show a large variety of interesting properties, like metal insulator transitions, colossal magnetoresistance, and superconductivity [1,2]. One reason for the complex behavior of these materials is the strong interplay between the orbital, charge, spin, and lattice degrees of freedom [3]. In the manganates, for example, the orbital and charge ordering could be related to the magnetoresistance [4]. For vanadium oxides it has been shown that the orbital occupation changes drastically at the metal insulator transition [5,6], and in the layered high temperature superconducting cuprates the two-dimensional electronic structure is intimately linked to the unoccupied $d_{x^2-y^2}$ orbital. More recently there is a lot of activity in using interface induced effects in transition metal oxides to strongly modify the physical properties [7,8].

Since the orbital degrees of freedom play an important role in all of these materials, it is highly desirable to have good experimental methods to determine the energy scale of the crystal or ligand field splitting and the local symmetry. In principle this can be done by optical spectroscopy [9]; however, these so-called *d-d* excitations are even parity, therefore optically forbidden and often completely masked by transitions involving small amounts of impurities or defects. The reason why some of these transitions are optically visible at all is due to simultaneous excitations of magnons or phonons. This results in an intensity typically 1000 times smaller than the intensity found for the close-by charge-transfer or Mott-Hubbard excitations. In multilayers and interfaces the problem is even more severe since there may be a variety of optical transitions due to other components that quickly mask out the *d-d* transitions. One is even not always able to easily discriminate between absorption peaks owing to *d-d* excitations also referred to as orbiton excitations and multiple phonon excitations, for example [10,11].

The last decade resonant inelastic x-ray scattering (RIXS) techniques have been developed to study *d-d* excitations. At the transition metal *K* edge a 1*s* to 4*p* excitation is involved. In the intermediate state the *d* levels shift due to the changed local potential. This energy shift can change the occupied *d* orbital wave function, which may result in a resonant enhancement of the *d-d* excitations [12–14]. The drawback of resonant scattering at the *K* edge is, however, that charge-transfer excitations are enhanced much more efficiently than the *d-d* [12,15] for two reasons. The first is that the 4*p* orbitals of the intermediate state are quite spatially extended and have a small interaction with the 3*d* orbitals but a very large one with the surrounding ligand orbitals. The second reason is that the *spherical* core hole potential does not enhance *d-d* transitions directly. Another option developed recently is RIXS at the transition metal $L_{2,3}$ edge or $M_{2,3}$ edge. Here one excites (and deexcites) a 2*p* or 3*p* transition metal core electron into the 3*d* valence shell. With this technique one can choose which of the low-lying energy states one wants to enhance by selecting the incident energy and polarization [12,16–18].

Recently, Larson *et al.* [19] observed clear *d-d* excitations within the gap in NiO and CoO with the use of nonresonant inelastic x-ray scattering (NIXS). In principle, one should expect that these excitations can be seen with NIXS, but surprisingly they found that the intensity of the *d-d* excitations at certain $\vec{q}$ vectors is much higher than the intensity of the charge-transfer or Mott-Hubbard excitations. They analyzed their experimental findings in the framework of LDA + U, which describes the transitions in terms of one particle interband transitions quite different from a transition involving strongly bound excitonic states as is known to be the case for these states in NiO and CoO. Very interesting to note though is that the angular dependent results can be quite well described within the band

257401-1

structure approach for the case of NiO because the transition involves basically a promotion of a t_{2g} electron into an unoccupied e_g state. In more complicated cases involving multi-Slater determinant excitonic bound states, the situation will be quite a bit more involved as also realized by the authors of that paper and previous work on the cuprates by Ku *et al.* [20].

In this Letter we will develop a local but many body treatment of NIXS and describe the observed *d-d* excitations within a configuration interaction cluster calculation analogous to the approaches used for analyzing the energy positions of optical *d-d* excitations [21] or the RIXS spectra at the $L_{2,3}$ edge [16,17]. The goal is to show that a straightforward and quantitative description of NIXS in the cases of excitonic excitations is possible. This description necessarily goes beyond the LDA + U approximation in order to describe local *d-d* excitations which do not involve U and are located inside the gap. To demonstrate the more general nature of this treatment we include some results for core 4*d*-4*f* and *f-f* transitions in Ce. More specific calculations and experimental results on Ce will be published elsewhere [22].

The interaction of matter with light is given by two terms. One proportional to the vector potential ($\vec{A}$) squared, the other proportional to the dot product of the momentum operator for the electrons ($\vec{p}$) with the vector potential.

$$H_{int} = \frac{e^2}{2m_e c^2}\vec{A}^2 + \frac{e}{m_e c}\vec{p}\cdot\vec{A}. \tag{1}$$

At resonance the second term ($\vec{p}\cdot\vec{A}$) is responsible for the largest contribution to the scattering cross section. Off resonance this term loses importance rapidly and the scattering is governed mainly by the term $\vec{A}^2$. The off resonance scattering cross section is then given by

$$\frac{d^2\sigma}{d\Omega d\omega_f} = r_0^2 \frac{\omega_f}{\omega_i}\sum_f |\vec{\epsilon}_i\cdot\vec{\epsilon}_f^*\langle f|e^{\iota(\vec{k}_i-\vec{k}_f)\cdot\vec{r}}|i\rangle|^2$$
$$\times \delta(E_i - E_f + \hbar(\omega_i - \omega_f)). \tag{2}$$

One can define the dynamical structure factor $S(\vec{q},\omega)$, which is a function of the scattering vector $\vec{q} = \vec{k}_i - \vec{k}_f$ and the energy loss $\omega = \omega_i - \omega_f$, as $S(\vec{q},\omega) = \frac{d^2\sigma}{d\Omega d\omega_f}/(r_0^2\frac{\omega_f}{\omega_i}|\vec{\epsilon}_i\cdot\vec{\epsilon}_f^*|^2)$, which has the advantage that all nonmaterial dependent factors are factored out.

$S(\vec{q},\omega)$ is a sum over transition probabilities multiplied by a delta function responsible for the energy conservation. This can be written as a Green's function in the spectral representation:

$$S(\vec{q},\omega) = \sum_f |\langle f|e^{\iota\vec{q}\cdot\vec{r}}|i\rangle|^2\delta(E_i - E_f + \hbar\omega)$$
$$= \lim_{\Gamma\to 0} -\frac{1}{\pi}\operatorname{Im}\langle i|T^\dagger\frac{1}{E_i - H + \hbar\omega + \frac{\iota\Gamma}{2}}T|i\rangle. \tag{3}$$

With the transition matrix equal to $T = e^{\iota\vec{q}\cdot\vec{r}}$.

To enable a rather direct symmetry analysis, we prefer to discuss the transitions in terms of monopole, dipole, quadrupole, etc., excitations, and in order to do so we expand the transition matrix on spherical harmonics.

$$e^{\iota\vec{q}\cdot\vec{r}} = \sum_{k=0}^\infty \sum_{m=-k}^k \iota^k(2k+1)j_k(qr)C_m^{(k)*}(\theta_q,\phi_q)$$
$$\times C_m^{(k)}(\theta_r,\phi_r)k \tag{4}$$

with $C_m^{(k)} = \sqrt{4\pi/(2k+1)}Y_{km}$, and $Y_{k,m}$ the spherical harmonics. This results in a sum over k of a spherical Bessel function of order k times a spherical harmonic of order k. Only terms with $k + l_f + l_i$ even and $|l_f - l_i| \le k \le l_f + l_i$ contribute, whereby l_i (l_f) is the angular momentum of the initial (final) state orbital involved. We first discuss the effect of changing the length of the $\vec{q}$ vector and then the effect of changing the orientation of the sample with respect to the $\vec{q}$ vector.

The expectation value of a spherical Bessel function is small if it oscillates strongly over the length scale of the product of the initial and final-state wave functions. We therefore expect the maximum intensity to occur at q values of length comparable to the atomic radial extent of the involved wave functions. In Fig. 1 we plot the expectation value of the spherical Bessel function for 3*d*-3*d* and 3*p*-3*d* excitations in Ni^{2+} and for 4*f*-4*f* and 4*d*-4*f* excitations in Ce^{3+}. The radial wave function has been calculated within the Hartree-Fock approximation with the use of Cowan's code [23]. Each of the different multipoles has a maximum at a different $\vec{q}$ vector. Concentrating on Ni^{2+} one sees that, for monopole excitations, one should use small wave vectors or forward scattering although a monopole transition contributes only to the zero energy loss peak because the excited states are orthogonal to the ground state as they are eigenfunctions of the same Hamiltonian. Quadrupole excitations become maximal around 6 Å^{-1}, and hexadecapole excitations become largest between 9 and 14 Å^{-1}. For most values of q one measures a mixture of quadrupole and hexadecapole tran-
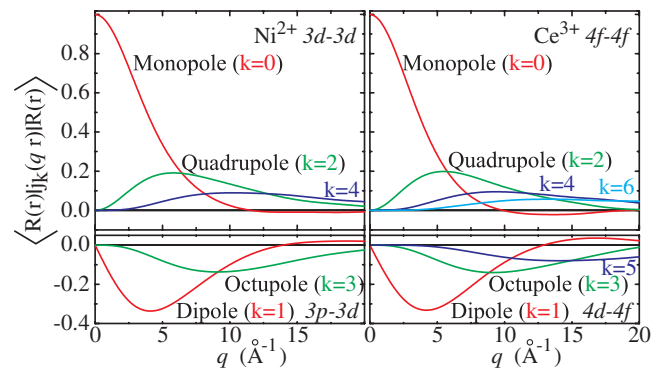

FIG. 1 (color online). Expectation value of the spherical Bessel function for several transitions as a function of q.

sitions. One should realize that there are interference terms between the different multipoles.

In Fig. 2(a) we show the NIXS spectra of NiO and CoO calculated for a TMO_6^{10-} cluster, with the use of the program XTLS8.3 [24,25]. A broadening of 120 meV has been included. For both NiO and CoO we see two peaks, with maximum intensity for $q = 7$ Å^{-1} in good agreement with the measurements of Larson *et al.* [19]. The *d-d* excitations are labeled by the symmetry of the final state without the inclusion of spin-orbit coupling. These peaks are split by spin-orbit coupling, as states of T symmetry are threefold orbital degenerate. In principle, higher resolution experiments are possible, and this splitting can be resolved. High-resolution (5 meV) calculations are shown in Fig. 2(b). Note that relative intensities of the different spin-orbit coupling split peaks depend on the orientation of the spin with respect to $\vec{q}$. These spectra have been calculated in cubic symmetry for a paramagnetic phase.

We now can compare these calculations to the *d-d* spectra found in optical spectroscopy [9] or RIXS [16] at the $L_{2,3}$ edge. The first thing one notices is that with optics and RIXS one sees many more *d-d* excitations than with NIXS. The explanation is straightforward if one considers the selection rules. For NIXS one has pure charge excitations and therefore the selection rule $\Delta S = 0$. For NiO, which has a ground state of $^3A_2$ symmetry with $t_{2g}^6 e_g^2$

configuration [26], there are three possible excited states that are also triplets, namely, two states of $^3T_1$ symmetry (around 1.8 and 3.0 eV) and one of $^3T_2$ symmetry (around 1.1 eV). One can see only two peaks as the $^3T_2$ state cannot be reached by a quadrupole excitation. The selection rules are rather different in RIXS at the $L_{2,3}$ edge. There one has an intermediate state with a core hole in the $2p$ shell of the transition metal. The spin-orbit coupling constant for $2p$-core electrons of Ni is around 11.5 eV and mixes states of different spins. This mixing results in different spin state transitions to be observed with comparable intensities in RIXS at the $2p$ edge.

In Fig. 2(c) we show the NIXS intensity of the 3.0 eV loss peak as a function of the magnitude of q. There are several ways in which one could change the magnitude of q. For the geometry as shown in the inset of Fig. 2, $|\vec{q}| = 2\cos(\phi)\frac{2\pi E}{hc}$, which means one can change the energy of the photons or change the scattering angle in order to change the magnitude of q. For convenience we show three different, equivalent scales for Fig. 2(c).

Another advantage of NIXS is that one can not only tune the magnitude of q in order to optimize the scattered intensity one can also use the directional dependence, i.e., the direction of the $\vec{q}$ vector with respect to the crystal axes in order to do something equivalent to polarization analyses. The transition matrix depends on the direction of the $\vec{q}$ vector by $\sum_{m=-k}^{k} C_m^{(k)*}(\theta_q, \phi_q) C_m^{(k)}(\theta_r, \phi_r)$. For a dipole transition ($k = 1$), for example, this is equivalent to a dipole in the direction of $\vec{q}$. This allows for a determination of the symmetry of the initial and the final states, based on selection rules. In the top panels of Fig. 3 we show the angular dependence for the NIXS intensity of different energy loss peaks of NiO and CoO at $q = 3.5$ Å^{-1} and $q = 7$ Å^{-1}. One can see that the two peaks of $^3T_1$ symmetry in NiO show the same angular dependence, whereas the two peaks in CoO, which are of different symmetry show a different angular dependence. It should be noted that the angular dependence calculated at $q = 3.5$ Å^{-1} for the peaks at 3.0 (2.36) eV energy loss of NiO (CoO) shows good agreement with the intensities as measured by Larson *et al.* [19]. It is interesting to note that the *d-d* excitation at 1.1 eV in NiO, which is not quadrupole allowed can be seen at $q = 7$ Å^{-1}, with the use of a hexadecapole transition. These are strongly peaked in approximately the [113] direction.

To conclude, we have expanded the nonresonant contribution (A^2) to the dynamical structure factor ($S(\vec{q}, \omega)$) in spherical harmonics. $S(\vec{q}, \omega)$ for CoO and NiO has been calculated with the use of this expansion. We used a configuration interaction cluster calculation, in order to describe the final-state excitons correctly. The calculated spectra are in excellent agreement with measurements of Larson *et al.* [19]. The spectral representation of $S(\vec{q}, \omega)$ presented here gives a straightforward explanation of the measured energy loss intensity. A big advantage is that $S(\vec{q}, \omega)$ in the multipole expansion is easy to calculate.
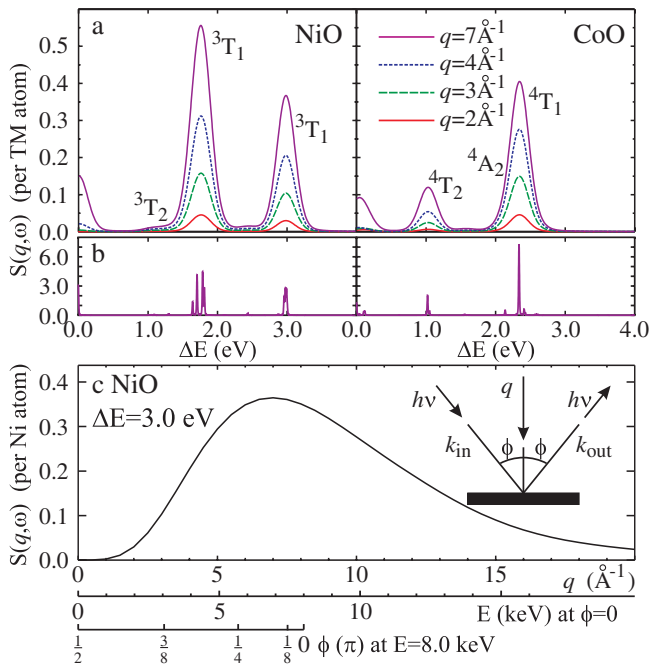
FIG. 2 (color online). (a) NIXS spectra for different values of q in the [111] direction calculated for a NiO$_6$ and a CoO$_6$ cluster. The monopole scattering has not been included. (b) High-resolution (5 meV) calculations showing the spin-orbit splitting of the different peaks. (c) NIXS intensity for the NiO peak at 3.0 eV loss calculated for different values of q. The photon energy at $\phi = 0$ and the scattering angle (ϕ) at a photon energy of 8 keV are given as alternative scales.
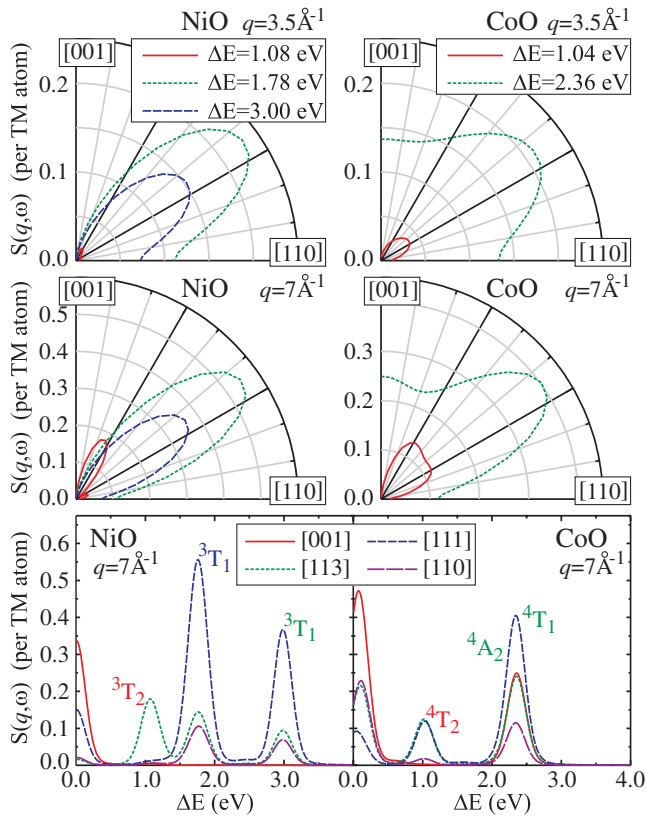
FIG. 3 (color online).   Top panels: Angular dependence of the NIXS intensity for NiO and CoO at different loss energies calculated at $q = 3.5$ Å^{-1} and at $q = 7$ Å^{-1}. Bottom panels: NIXS spectra at $q = 7$ Å^{-1} for different sample orientations.

This is especially suitable for excitonic excitations with q values comparable to atomic dimensions. For other excitations involving interband transitions and collective modes, one could rely on local-density approximation or time dependent density-functional theory [27–29]. By changing the magnitude of q, one can tune the sensitivity of the measurement to different multipoles and optimize the intensity of the d-d excitation. A certain multipole has optimal intensity if the spherical Bessel function of the same order has a period comparable to the size of the local d orbital. Rotating the sample with respect to the $\vec{q}$ vector allows one to do something equivalent to polarization analysis. This creates the opportunity to determine the symmetry of the ground state and excited state with the use of selection rules. It is important to note that this kind of measurement is bulk sensitive and can be used to study buried interfaces. The elemental sensitivity is not as strong as in RIXS, but because the radial matrix elements depend on the radial extent of the d wave functions some degree of elemental sensitivity remains. For Ni one finds, for example, a maximum quadrupole intensity at $q \approx 6$ Å^{-1}, whereas for Ti this intensity is maximum at $q \approx 4$ Å^{-1}. We believe that this kind of measurement can provide important information on the electronic structure and local

symmetry of some of the most fascinating strongly correlated rare earth and transition metal compounds.

[1] N. Tsuda *et al.*, *Electronic Conduction in Oxides* (Springer-Verlag, Berlin, 2000).

[2] M. Imada, A. Fujimori, and Y. Tokura, Rev. Mod. Phys. **70**, 1039 (1998).

[3] See, for example, the contributions to the Focus on Orbital Physics, New J. Phys. 6 (2004).

[4] Y. Tokura and N. Nagaosa, Science **288**, 462 (2000).

[5] J.-H. Park *et al.*, Phys. Rev. B **61**, 11506 (2000).

[6] M. W. Haverkort *et al.*, Phys. Rev. Lett. **95**, 196404 (2005).

[7] A. Ohtomo and H. Y. Hwang, Nature (London) **427**, 423 (2004).

[8] S. Okamoto and A. J. Millis, Nature (London) **428**, 630 (2004).

[9] R. Newman and R. M. Chrenko, Phys. Rev. **114**, 1507 (1959).

[10] E. Saitoh *et al.*, Nature (London) **410**, 180 (2001).

[11] M. Grüninger *et al.*, Nature (London) **418**, 39 (2002).

[12] A. Kotani and S. Shin, Rev. Mod. Phys. **73**, 203 (2001).

[13] J. van der Brink and M. van Veenendaal, J. Phys. Chem. Solids **66**, 2145 (2005).

[14] P. M. Platzman and E. D. Isaacs, Phys. Rev. B **57**, 11107 (1998).

[15] C.-C. Kao, W. A. L. Caliebe, J. B. Hastings, and J.-M. Gillet, Phys. Rev. B **54**, 16361 (1996).

[16] G. Ghiringhelli *et al.*, J. Phys. Condens. Matter **17**, 5397 (2005).

[17] M. Magnuson, S. M. Butorin, J.-H. Guo, and J. Nordgren, Phys. Rev. B **65**, 205106 (2002).

[18] P. Kuiper *et al.*, Phys. Rev. Lett. **80**, 5204 (1998).

[19] B. C. Larson *et al.*, Phys. Rev. Lett. **99**, 026401 (2007).

[20] W. Ku, H. Rosner, W. E. Pickett, and R. T. Scalettar, Phys. Rev. Lett. **89**, 167204 (2002).

[21] G. J. M. Janssen and W. C. Nieuwpoort, Int. J. Quantum Chem. **34**, 679 (1988).

[22] R. A. Gordon *et al.*, Europhys. Lett. **81**, 26004 (2008).

[23] R. D. Cowan, *The Theory of Atomic Structure and Spectra* (University of California Press, Berkeley, 1981).

[24] A. Tanaka and T. Jo, J. Phys. Soc. Jpn. **63**, 2788 (1994).

[25] The parameters used for the cluster calculations are similar to the ones used for the RIXS calculations [16].

[26] C. J. Ballhausen, *Ligand Field Theory* (McGraw-Hill Book Company, Inc., New York, 1962).

[27] S. Doniach, P. M. Platzman, and J. T. Yue, Phys. Rev. B **4**, 3345 (1971).

[28] S. Galambosi *et al.*, Phys. Rev. B **64**, 024102 (2001).

[29] A. G. Eguiluz *et al.*, J. Phys. Chem. Solids **66**, 2281 (2005).